1-16-2014

Mutation of A DNA Repair Enzyme Causes Lupus in Mice

Ali Senejani
University of New Haven, asenejani@newhaven.edu

Yanfeng Liu
Yale University

Dawit Kidane
Yale University

Stephen E. Maher
Yale University

Caroline J. Zeiss
Yale University

See next page for additional authors

Publisher Citation

Senejani A.G., Liu Y., Kidane D., Maher S.E., Zeiss C.J., Park H., Kashgarian M., McNiff J.M., Zelterman D., Bothwell A., Sweasy J.B. "Mutation of A DNA Repair Enzyme Causes Lupus in Mice" Cell reports (CELL PRESS) 2014 Jan 16;6(1):1-8. doi:10.1016/j.celrep.2013.12.017.

Cell Reports
Report

Mutation of *POLB* Causes Lupus in Mice

Alireza G. Senejani,[1,2] Yanfeng Liu,[2] Dawit Kidane,[1,2] Stephen E. Maher,[3] Caroline J. Zeiss,[4] Hong-Jae Park,[5] Michael Kashgarian,[6] Jennifer M. McNiff,[7] Daniel Zelterman,[8] Alfred L.M. Bothwell,[3] and Joann B. Sweasy[1,2,*]
[1]Department of Therapeutic Radiology, Yale School of Medicine, New Haven, CT 06520, USA
[2]Department of Genetics, Yale School of Medicine, New Haven, CT 06520, USA
[3]Department of Immunobiology, Yale University School of Medicine, New Haven, CT 06520, USA
[4]Section of Comparative Medicine, Yale University School of Medicine, New Haven, CT 06510, USA
[5]Department of Life Science, Hanyang University, Seoul 133-791, Republic of Korea
[6]Department of Pathology, Yale University School of Medicine, New Haven, CT 06520-8023, USA
[7]Department of Dermatology, Yale University School of Medicine, New Haven, CT 06520-8023, USA
[8]School of Public Health, Yale University School of Medicine, New Haven, CT 06520-8034, USA
*Correspondence: joann.sweasy@yale.edu
http://dx.doi.org/10.1016/j.celrep.2013.12.017

SUMMARY

A replication study of a previous genome-wide association study (GWAS) suggested that a SNP linked to the *POLB* gene is associated with systemic lupus erythematosus (SLE). This SNP is correlated with decreased expression of Pol β, a key enzyme in the base excision repair (BER) pathway. To determine whether decreased Pol β activity results in SLE, we constructed a mouse model of POLB that encodes an enzyme with slow DNA polymerase activity. We show that mice expressing this hypomorphic POLB allele develop an autoimmune pathology that strongly resembles SLE. Of note, the mutant mice have shorter immunoglobulin heavy-chain junctions and somatic hypermutation is dramatically increased. These results demonstrate that decreased Pol β activity during the generation of immune diversity leads to lupus-like disease in mice, and suggest that decreased expression of Pol β in humans is an underlying cause of SLE.

INTRODUCTION

Base excision repair (BER) functions during class switch recombination (CSR) and somatic hypermutation (SHM) (for a review, see Alt et al., 2013). Although BER is mainly known for its function in the repair of at least 20,000 endogenous base lesions per human cell per day (Barnes and Lindahl, 2004), it appears to have been co-opted from this role to act in the generation of antibody diversity (for a review, see Di Noia and Neuberger, 2007). DNA polymerase beta (Pol β) is a key protein in the BER pathway, where it repairs single-strand breaks. Deletion of the *POLB* gene from mice results in embryonic lethality (Gu et al., 1994).

In a large-scale replication study based upon a previous genome-wide association study (GWAS) of SLE in the Han Chinese population, association evidence for rs12676482 with systemic lupus erythematosus (SLE) was replicated independently in two large cohorts (Sheng et al., 2011). The significance of this lies in the fact that rs12676842 is a SNP in the noncoding region adjacent to the *POLB* gene on 8p11.21. Of note, the lupus-associated SNP rs12676482 is in perfect linkage disequilibrium with rs2272733, which is highly correlated with decreased *POLB* expression (Zeller et al., 2010). This suggests that low Pol β activity is an underlying cause of SLE. We reasoned that mice expressing a slow Pol β mutant polymerase, such as the Y265C hypermorphic allele, would be an excellent model to test the hypothesis that limiting the levels of active Pol β leads to SLE. The Y265C mutant of *POLB* encodes a protein that synthesizes DNA significantly more slowly than wild-type (WT) Pol β (Washington et al., 1997). Therefore, we constructed a $POLB^{Y265C/C}$ mouse model using targeted gene disruption (Senejani et al., 2012). We demonstrate that these mice exhibit several pathologies associated with SLE. In addition, our strategy allowed us to define the contributions of Pol β during V(D)J recombination and SHM. Importantly, our studies suggest that an imbalance of error-prone and error-free break repair during V(D)J recombination and SHM results in autoimmune disease.

RESULTS

$POLB^{Y265C/C}$ Mice Have Pathologies Resembling SLE

We previously constructed the $POLB^{Y265C/C}$ mouse model using targeted gene disruption (Senejani et al., 2012). Observation of the mice as they aged revealed an intriguing set pathologies resembling SLE. The $POLB^{Y265C/C}$ and $POLB^{Y265C/+}$ mice exhibited an increased prevalence of dermatitis (Figures 1A and S1). Dermatitis is a major manifestation of SLE in humans (Norris and Lee, 1985) and is also observed in the SLE-prone MRL/lpr lupus-like mouse model (Furukawa et al., 1984). The $POLB^{Y265C/+}$ and $POLB^{Y265C/C}$ mice exhibited significantly increased levels of antinuclear antibodies (ANAs) in their blood sera compared with WT mice, and the ANA levels continued to rise over the lifetime of the mice (Figure 1B).

Besides ANA, another hallmark feature of SLE is glomerular nephritis (Radic et al., 2011), which results from the formation

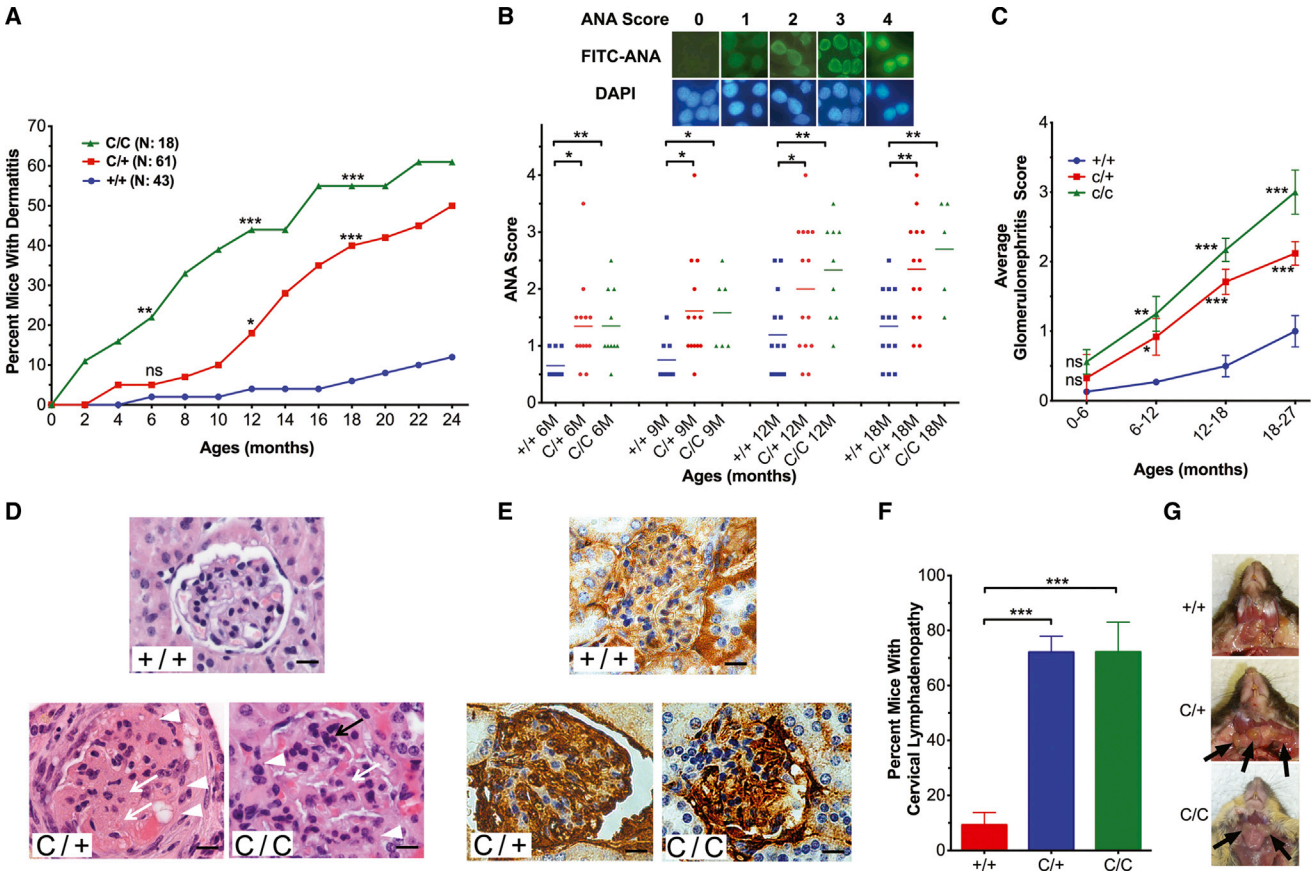

Figure 1. *POLB*$^{Y265c/c}$ and *POLB*$^{Y265c/+}$ Mice Exhibit Multiorgan Symptoms of SLE

(A) Levels of lupus-like dermatitis are increased significantly in *POLB*$^{Y265c/c}$ and *POLB*$^{Y265c/+}$ mice compared with WT mice as the mice age. Shown are curves for each genotype (*POLB*$^{+/+}$, *POLB*$^{c/+}$, and *POLB*$^{c/c}$) representing the percentage of mice with lupus-like dermatitis.

(B) *POLB*$^{Y265c/c}$ and *POLB*$^{Y265c/+}$ mice have higher levels of ANA than WT mice. Shown above the graph is an example of immunofluorescence intensity in 12-month-old mutant mice compared with their WT littermates and MRL/lpr mice. Note that the fluorescence pattern observed in the MRL/lpr mice differs from that observed in the *POLB*$^{Y265c/c}$ and *POLB*$^{Y265c/+}$ mice. In the graph, levels of ANA were quantified from several mice (WT, blue squares; c/+, red circles; c/c, green triangles) at various ages. In brief, ANA was tested by immunofluorescence using human epithelial (*HEp-2*) cells in 12-well slides (Diasorin). For each run, 1:50 diluted sera were used in a screening investigation. Samples from mice with high and low ANA scores were used on the same slide to confirm the sensitivity and specificity of the test during each scoring.

(C) *POLB*$^{Y265c/c}$ and *POLB*$^{Y265c/+}$ mice exhibit increased severity of glomerular nephritis compared with WT mice. The severity of kidney lesions was scored from 0 to 3 for normal, mild, moderate, or severe, respectively. For each mouse, more than ten glomerular, tubular, or interstitial areas were evaluated and scored for glomerular cellularity, infiltrating leukocytes, severity of tubular lesions, mesangial matrix expansion, crescent formation, and interstitial mononuclear cell infiltrates in the medulla and cortex. Lesion scores for each mouse were calculated as the mean of the summed individual scores from each evaluated factors.

(D) Examples of renal disease in *POLB*$^{Y265c/c}$ mice compared with WT. The black arrow points to mesangial hypercellularity. The white arrow denotes basement membrane thickening, and white arrowheads indicate glomerular crescents. The gray arrow denotes deposits of antibodies, and the black arrow indicates shrunken glomeruli in the outer cortex.

(E) The kidneys of *POLB*$^{Y265c/c}$ mice exhibit significantly more intense IgG staining than those of WT mice.

(F) *POLB*$^{Y265c/c}$ mice exhibit significantly increased levels of cervical lymphadenopathy compared with WT mice.

(G) Examples of enlarged cervical lymph nodes in *POLB*$^{Y265c/c}$ and *POLB*$^{Y265c/+}$ mice compared with the normal nodes shown in the WT mouse. Arrows point to the cervical lymph nodes.

The error bars represent the SEM for the results of at least three experiments, and p values were calculated using the unpaired t test.

of immune complexes on the kidneys. The *POLB*$^{Y265C/+}$ and *POLB*$^{Y265C/C}$ mice developed significantly increased levels of glomerular nephritis compared with WT mice (Figure 1C). By 12 months of age, we observed increased levels of immunoglobulin G (IgG) localized to the glomeruli of the *POLB*$^{Y265C/C}$ mice versus WT controls (Figure 1E). Approximately 70% of the *POLB*$^{Y265C/+}$ and *POLB*$^{Y265c/c}$ mice exhibited cervical lymphadenopathy (Figures 1F–1G) with significant infiltration of T and B lymphocytes (Figure S2), which are recognized symptoms of SLE (Jonsson et al., 1987; Lavoie et al., 2011). In contrast, few of their WT siblings had enlarged cervical lymph nodes. Several of the mutant mice also exhibited enlarged salivary glands that had infiltrating lymphocytes, which were predominantly T and B cells (Figure S3). In combination, our results are consistent with the interpretation that expression of a low-activity Pol β variant leads to lupus-like disease in mice.

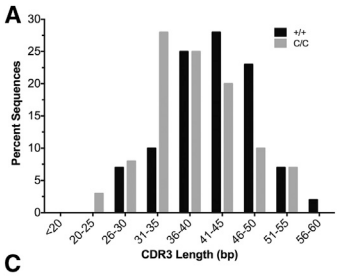

B

CDR3 Length of Heavy Chain ($V_{H81X}DJ_{H4}$) Rearrangements in *POLB* $Y265^{C/C \text{ and } +/+}$ Mice

Tissue	*POLB*	CDR3 Length in bp (Number of Sequences) In frame Seqences	Out of frame Sequences	Total Sequences	CDR3 Size Range in bp
Spleen	$Y265^{+/+}$	40.83(18)	43.87 (15)	42.21 (33)	27-60
	$Y265^{C/C}$	37.5 (25)	35.9 (17)	37.88 (42)	24-52
Bone Marrow	$Y265^{+/+}$	40.50 (14)	41.64 (14)	41.07 (28)	29-53
	$Y265^{C/C}$	36.46 (13)	39.22 (9)	37.59 (22)	22-53

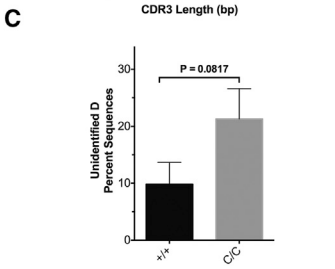

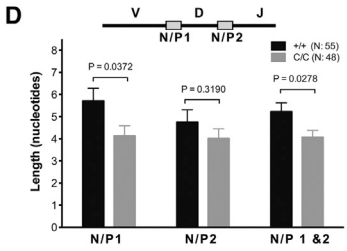

Figure 2. VDJ Recombination Is Aberrant in *POLB*$^{Y265c/c}$ Mice

(A) PCR-amplified products from B220^{+} IgM^{-} bone marrow and splenic cell genomic DNA of 3- to 4-week-old *POLB*$^{+/+}$ and *POLB*$^{C/C}$ mice were cloned and sequenced. The lengths of the CDR3 sequences as a function of the percentage of sequences with particular lengths are plotted in the graph. Note that the majority of CDR3 sequences from the *POLB*$^{Y265c/c}$ mice have a length of 31–35 bases, whereas the CDR3 region of WT mice is 41–45 bases in length. At least three mice of each genotype were characterized.

(B) The table shows the ranges of lengths of the CDR3 regions from spleen and bone marrow found in WT and *POLB*$^{Y265c/c}$ mice.

(C) The percentage of D regions in the *POLB*$^{C/C}$ mice that were unidentifiable was significantly greater than that observed in WT controls. D regions were identified on the basis of six contiguous nucleotides.

(D) The average length of N/P-nucleotide addition was reduced in *POLB*$^{C/C}$ mice. The allocation of N/P nucleotides was based on the known sequences of the germline elements. The average length of the N/P region between the rearranged V and D junction (N1) was significantly shorter in *POLB*$^{C/C}$ mice compared with WT controls. The N/P region between the rearranged D and J junction (N2) was not significantly different between *POLB*$^{+/+}$ and *POLB*$^{C/C}$ mice.

The error bars represent the SEM for the results of at least three experiments, and p values were calculated using the unpaired t test.

The CDR3 Junctions of the Heavy Chains Are Short in *POLB*$^{Y265c/c}$ Mice

To determine whether the process of V(D)J recombination was altered in our mice, we sequenced the V-D and D-J junctions of T and B cell receptors from the WT and *POLB*$^{Y265C/C}$ mice, and found that the B cells derived from mutant mice had shorter CDR3 junctions in the Ig heavy chain compared with those from the WT (Figures 2A, 2B, and S4). The majority of CDR3 junctions in the *POLB*$^{Y265C/C}$ mice were 31–35 base pairs in length, whereas they were 41–45 base pairs in the WT mice (Figure 2A), with many more unidentifiable D regions in the mutant versus WT mice (Figure 2C; Bertocci et al., 2006). The lengths of N/P additions between the rearranged V and D segments were significantly shorter in the *POLB*$^{Y265C/C}$ mice than in WT controls ($p < 0.05$; Figure 2D). No significant differences in length of the Ig light chain junctions or the T cell receptors were observed (data not shown). Thus, the slow polymerase activity of the Y265C variant leads to fewer N/P additions between the rearranged V and D segments of the Ig heavy chain.

CSR Is Similar in WT and *POLB*$^{Y265C/C}$ Mice

Previous work suggested that Pol β functions in CSR (Wu and Stavnezer, 2007). In that study, fetal liver cells isolated from WT or *POLB*$^{\Delta/\Delta}$ mice were transplanted into irradiated hosts, and in vitro CSR assays showed slight increases in switching to IgG2a. As shown in Figure 3, we observed no differences in the levels of IgG1, IgG2a, IgG2b, or IgG3 in the *POLB*$^{Y265C/C}$ versus WT mice, suggesting that CSR is not altered in the Pol β mutant mice.

The Rate of SHM Is Significantly Higher in *POLB*$^{Y265C/C}$ Mice

SHM is a co-opted form of BER and occurs in later stages of B cell development within the germinal center (GC) (Di Noia and Neuberger, 2007; Maul and Gearhart, 2010; Victora and Nussenzweig, 2012). SHM occurs primarily in the variable region of the Ig heavy chain, which results in the production of high-affinity antibodies (Di Noia and Neuberger, 2007; Liu and Schatz, 2009; Rajewsky et al., 1987; Weigert et al., 1970). Because Y265C Pol β is a very slow BER polymerase, gaps in DNA that are generated during SHM are unlikely to be filled efficiently during SHM in the *POLB*$^{Y265C/C}$ mice. To determine whether this was the case, we characterized SHM in the J_{H4} intron downstream of $V_{HJ}558$-J_{H4} using PCR followed by DNA sequencing. Our analysis revealed that the *POLB*$^{Y265C/C}$ mice exhibited a significantly increased frequency of SHM compared with WT (Figures 4A and 4B). The frequencies of transversions at GC

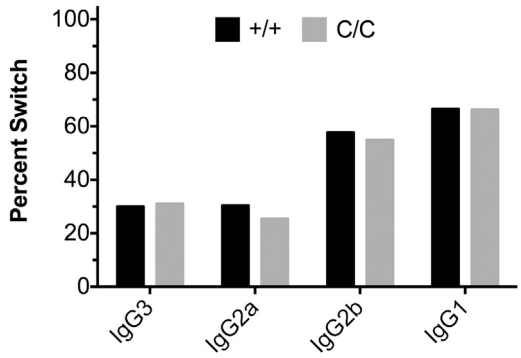

Figure 3. CSR Is Normal in *POLB*$^{Y265c/c}$ Mice

Naive splenic B cells were isolated from spleens of three to five *POLB*$^{Y265C/C}$ and WT control mice, and induced in vitro with either LPS to induce switching to IgG1, LPS with IL-4 to induce switching to IgG3, LPS with INFγ to induce switching to IgG2a, or LPS with TGFβ to induce switching to IgG2b. No significant change in CSR in the B cells was observed between the *POLB*$^{Y265C/C}$ and WT mice.

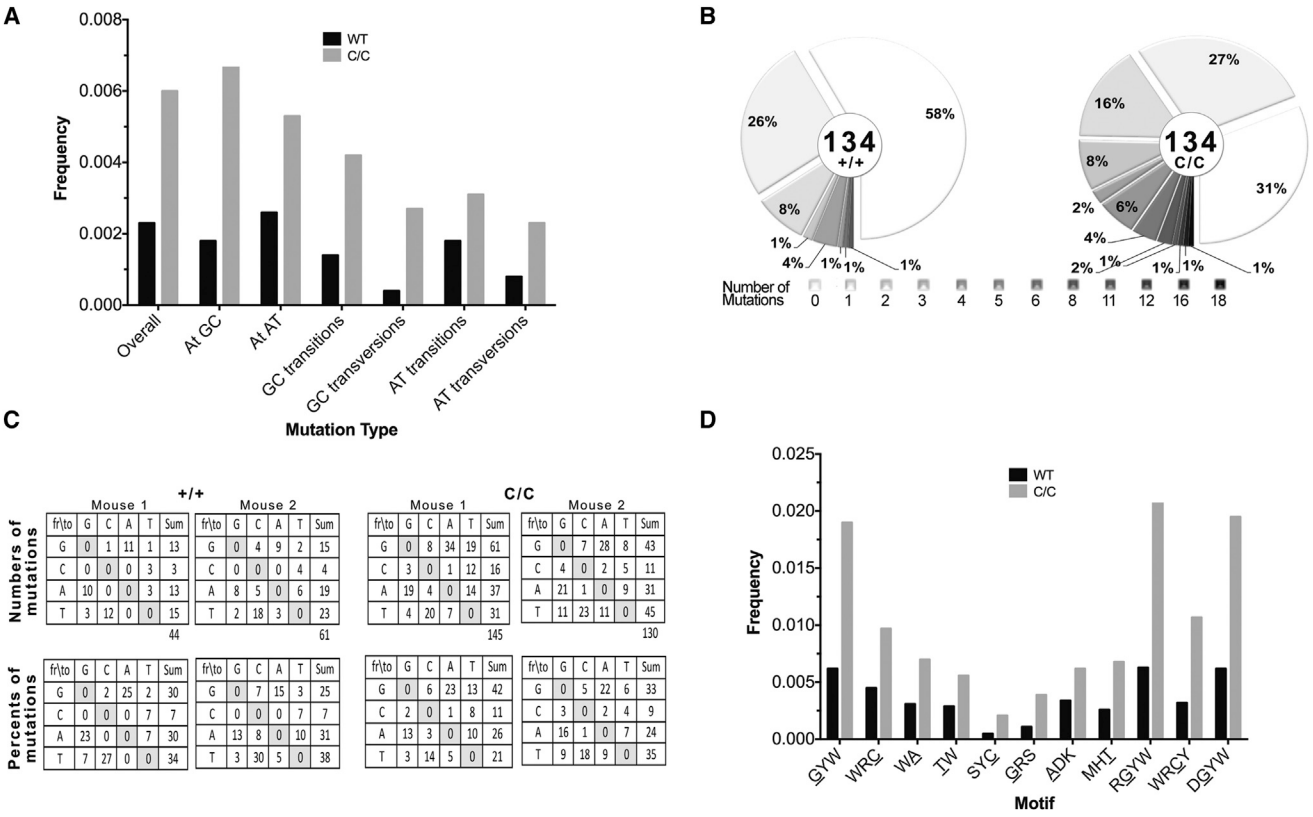

Figure 4. The Rate of SHM Is Increased in *POLB*$^{Y265c/c}$ Mice

(A) Products were amplified using PCR and genomic DNA isolated from B220^{+} PNA^{high} Peyer's patches of 3- to 5-month-old *POLB*$^{+/+}$ and *POLB*$^{C/C}$ mice. These products were cloned and sequenced. SHM results show that the overall frequencies are increased in the *POLB*$^{Y265c/c}$ mice compared with the WT.

(B) For SHM, the 344 nucleotides downstream of the J_{H4} gene region of rearranged VDJ segments on the heavy-chain locus of the VHJ558 gene were PCR amplified and sequenced. The numbers of mutations versus the total length of DNA sequences and the mutation frequency were analyzed in three mutant mice and three age-matched WT animals with the use of SHMTool, which is a webserver for comparative analysis of SHM data sets. At the center of the pie chart is shown the numbers of clones analyzed for each genotype. Segments show the percentage of each clone that contained a defined number of mutations, and these are indicated with different colors.

(C) All types of mutations are increased ($p = 3.7 \times 10^{-18}$) in the J_{H4} intron from the *POLB*$^{Y265c/c}$ mice, but the types of mutations that are most significantly increased are transversions at GC base pairs ($p = 2.8 \times 10^{-8}$), followed by transitions at GC ($p = 7.0 \times 10^{-7}$), transversions at AT ($p = 3 \times 10^{-5}$), and transitions at AT base pairs ($p = 0.0029$). At least three mice of each genotype were used for these experiments.

(D) Amino acid motifs shown on the x axis are where many of the SHM mutations occur in the *POLB*$^{Y265c/c}$ mice. Mutations arise predominantly in GYW ($p = 7.4 \times 10^{-5}$), RGYW ($p = 0.0003$), and DGYW ($p = 7.4 \times 10^{-5}$), which are the motifs in which deamination catalyzed by AID occurs.

The error bars represent the SEM for the results of at least three experiments, and p values were calculated using the unpaired t test.

base pairs were most significantly increased (Figures 4A and 4C), although increases in mutations at A:T base pairs were also elevated. The *POLB*$^{Y265C/C}$ mice also displayed increased levels of mutation in the hotspot motifs that are targeted by activation-induced cytidine deaminase (AID; Figure 4D).

Increased Numbers of GCs in *POLB*$^{Y265C/C}$ Mice

The increased frequencies of SHM in *POLB*$^{Y265C/C}$ mice prompted us to determine whether these mice possess increased numbers of GCs, as is often found in lupus-prone mice. The *POLB*$^{Y265C/C}$ mice exhibited increased numbers of GCs in spleen (Figure 5A). This observation is supported by a fluorescence-activated cell sorting (FACS) analysis that showed elevated numbers of GC B cells and follicular T helper cells (T_{FH}) in the spleens of *POLB*$^{Y265C/C}$ mice compared with WT mice (Figure 5B). However, there were significantly higher levels of apoptosis in the spleens of the *POLB*$^{Y265C/C}$ mice compared with WT mice (Figure 5C). To determine whether cell death was occurring in the GCs, we performed a terminal deoxynucleotidyl transferase dUTP nick end labeling (TUNEL) analysis. The *POLB*$^{Y265C/C}$ mice exhibited significantly increased levels of TUNEL-positive cells that mostly overlapped with CD4 T helper cells (Figures 5D and 5E).

DISCUSSION

Here, we show that mice carrying the Y265C hypomorphic allele of *POLB* develop several SLE-associated pathologies, suggesting that low activity of Pol β leads to SLE. Our results suggest that this phenotype arises as a result of aberrant V(D)J recombination and a high frequency of SHM. Our findings strongly implicate Pol β as a critical player in both V(D)J recombination and SHM.

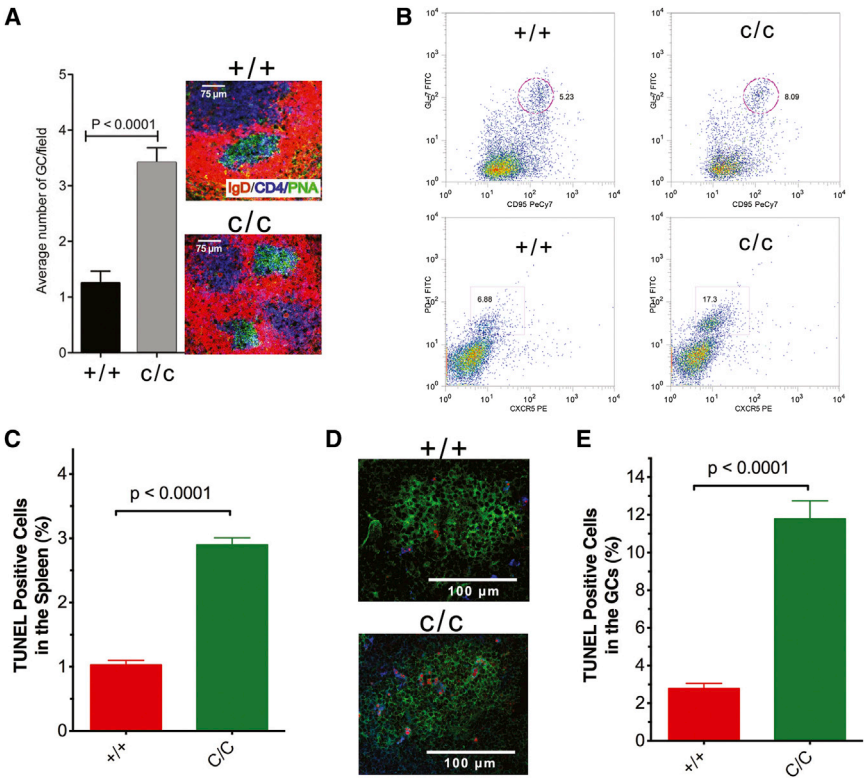

Figure 5. *POLB*$^{Y265c/c}$ Mice Have Increased Numbers of GCs Compared with WT Mice

(A) Spleens of three or four 5-month-old mice were frozen with OCT compound, prepared as a frozen section, and stained overnight at 4°C for confocal analysis. PNA-positive GCs were counted per field (25×). The graph compares the numbers of GCs in *POLB*$^{Y265c/c}$ and WT mice, and the image depicts an example of multiple GCs in the spleen of a *POLB*$^{Y265c/c}$ mouse.

(B) Examples of FACS-sorted splenic cells. For flow cytometry, splenic cells from three to five 5-month-old mice were processed and stained with anti-mouse antibodies (eBioscience) as described in the Supplemental Experimental Procedures. Top: GC B cells from a 5-month-old mouse were CD19^{+}IgD-lo gated, followed by gating for CD95 GI7 double-positive cells (WT (+/+) is on the left and c/c is on the right). Bottom: T_{FH} cells were CD4+ CD44-lo gated, followed by gating for CXCR5 PD-1 double-positive cells.

(C) Graph showing the percentage of TUNEL-positive cells from *POLB*$^{Y265c/c}$ and WT spleens, which is representative of at least three mice of each genotype.

(D) Spleen frozen sections were stained overnight at 4°C for confocal analysis. The image represents an example of GCs in the spleens of *POLB*$^{Y265c/c}$ and WT mice. PNA-positive GCs are shown in green (fluorescein isothiocyanate), CD4-positive T helper cells are shown in blue (αCD4-Cy5), and TUNEL-positive cells are shown in red.

(E) Graph showing the percentage of TUNEL-positive cells in the GCs of *POLB*$^{Y265c/c}$ and WT mice, which is representative of eight to ten GCs of two to three mice of each genotype.

Processing by *POLB*$^{Y265C/C}$ Leads to Short CDR3 Junctions During V(D)J Recombination

SLE is a classic autoimmune disease that is characterized by the production and circulation of ANAs that participate in tissue destruction. We have shown that *POLB*$^{Y265C/C}$ mice produce significantly higher levels of ANA than WT mice by 6 months of age, and that the levels of ANA continue to increase over the lifetime of the mice, leading to glomerulonephritis, dermatitis, and cervical lymphadenopathy. Because the production of ANA is a major causative factor of SLE, and because DNA repair proteins are central players in development of the lymphocyte repertoire, we investigated the potential role of Pol β Y265C in that process, starting with VDJ recombination. We showed that the CDR3 junctions of IgH, especially the N/P additions between the V and D fragments, are shorter in the *POLB*$^{Y265C/C}$ mice than in the WT. A model depicting the role of Pol β Y265C in joining the V and D fragments is shown in Figure 6. After cleavage by RAG proteins, hairpins are formed and cut by the Artemis endonuclease. If the incision by Artemis results in staggered ends, as shown in Figure 6, a DNA polymerase fills the gap, followed by ligation. When Y265C is present, gap filling is slow and inefficient, leading to nuclease activity that results in a shorter CDR3 junction. We suggest that Y265C Pol β acts in a dominant-negative manner by not permitting access of other DNA polymerases, including Pol λ and Pol μ, to the gapped DNA, eliminating functional redundancy. We point out that short gaps are the optimum DNA substrate for Pol β (Chagovetz et al., 1997). Previous work using mice deleted of the *POL L* gene provided evidence that Pol λ processes this gap (Bertocci et al., 2006). Characterization of V(D)J recombination in the absence of Pol β was not possible because *POLB*$^{Δ/Δ}$ mice do not survive past birth. In vitro reconstitution studies (Ma et al., 2004) did not demonstrate a role for Pol β. However, in these studies, Pol β was never assessed in combination with terminal transferase, Pol λ, and/or Pol μ, so its participation may not have been detected.

The Presence of *POLB*$^{Y265C/C}$ Does Not Alter CSR

CSR occurs by a process of intrachromosomal deletion that is initiated by the formation of double-strand breaks (DSBs). DSB formation is initiated when AID deaminates cytosine on both strands of the DNA in the switch regions. The resulting uracil residues are recognized and excised by uracil DNA glycosylase (UNG), followed by apurinic/apyrimidinic endonuclease 1 (APE1) incision (for a review, see Stavnezer et al., 2008). If the uracils are clustered and on opposite strands of the DNA, incision by APE1 will result in DSBs. Alternatively, the U:G mispair will be recognized by mismatch repair proteins that recruit exonuclease I (Exo I) to the DNA. Exo 1 excision opposite a nick that results from incision by APE1 can also result in a DSB. Therefore, gap filling by Pol β can prevent the formation of DSBs during CSR, as suggested previously when a slight increase in switching to

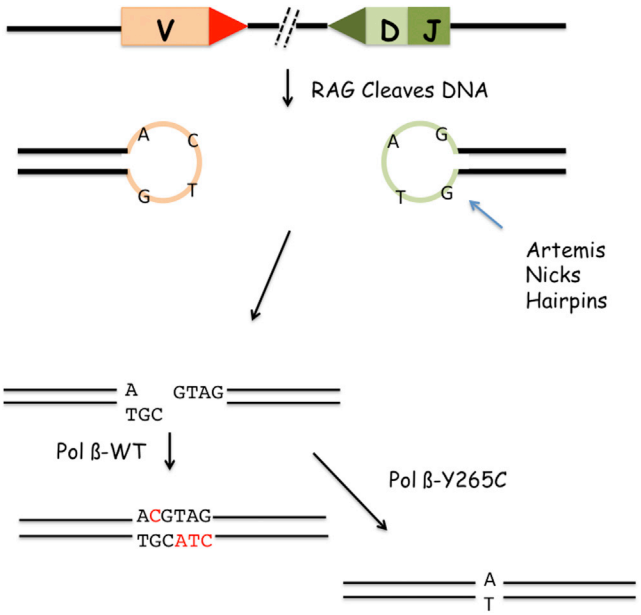

Figure 6. Model of Aberrant V(D)J and SHM in *POLB*$^{Y265c/c}$ Mice
Y265C Pol β promotes deletion during joining of the V and D fragments. This cartoon depicts joining of the V to the D fragment. After the Rag proteins cleave the DNA, hairpins form. Artemis nicks the hairpins, which sometimes results in a substrate with DNA gaps. WT Pol β or other X family polymerases fill the gaps. However, in the presence of the slow Y265C Pol β polymerase, gaps are filled inefficiently, which can result in nuclease activity leading to deletions and shortening of the CDR3 junction.

IgG2a was observed in *POLB*$^{\Delta/\Delta}$ B cells (Wu and Stavnezer, 2007). In contrast, we observed no significant increases in CSR in the B cells from *POLB*$^{Y265C/C}$ mice that were induced to switch in vitro. One explanation for our results is that the presence of the Y265C Pol β polymerase prevents significant DSB formation through the APE1 pathway because it has the ability to bind to and slowly fill the DNA gap. This suggests that mismatch repair could constitute a major DSB-formation pathway during CSR. The binding of Y265C Pol β to the 3′OH of the gap could also prevent further processing by nucleases.

Lack of Gap Filling by Y265C Pol β Results in Increased SHM

We showed that the frequency of SHM in the *POLB*$^{Y265C/C}$ mice was significantly increased over that of WT mice, and we observed increases predominantly in transversions at AID hotspots. These findings are consistent with the idea that Pol β plays a critical role in maintaining a balance between error-free and error-prone repair during SHM. A model for the role of Pol β Y265C is presented in Figure 7. After AID deaminates cytosine to uracil, there are three pathway choices. If replication occurs, transitions are observed at AID deamination hotspots. If the U:G mismatch is recognized by the mismatch repair pathway, mutations at A:T base pairs are observed. Alternatively, UNG removes uracil. Bypass of the resulting AP site by a translesion polymerase leads to transversions at the AID hotspot. However, should APE1 incise the backbone, a single nucleotide gap could be filled in by a translesion polymerase, resulting in transversions, or the gap could be filled in by Pol β in the canonical BER pathway, resulting in error-free repair. We suggest that gap filling is slow in the presence of Y265C Pol β, which would eventually lead to gap filling by TLS polymerases and the transversions we observe during SHM. Alternatively, Y265C could fill the gap in an error-prone manner. We do not favor this explanation, however, because we do not observe increased levels of transversions at G:C base pairs in in vivo or in vitro studies with Y265C Pol β (Clairmont et al., 1999; Opresko et al., 1998; Washington et al., 1997). Another possibility is that many gaps remain unfilled, eventually resulting in cell death, consistent with our observation of increased TUNEL foci in the spleens of the *POLB*$^{Y265C/C}$ mice. We note that in addition to increased levels of mutation at G:C base pairs, we also observe increases of A:T mutations. This could occur if the unfilled gap is bound by a nuclease, which would enlarge the gap. Filling of the larger gap by a translesion polymerase would lead to mutations at A:T base pairs.

Our findings are significant because they show that a balance between error-prone and error-free repair during SHM is critical, and that Pol β plays an important role in maintaining this balance. Our results suggest that too much mutagenesis during SHM has the potential to lead to autoimmune disease. In support of this suggestion, reversion of the mutations produced during SHM results in antibodies that no longer have antinuclear activity, suggesting that SHM itself is one mechanism for creating autoreactive antibodies (Guo et al., 2010; Wellmann et al., 2005).

Selection in the GC?

Not only do the *POLB*$^{Y265C/C}$ mice have increased numbers of GCs, but the GCs exhibit significantly increased TUNEL staining compared with WT mice. Gaps that arise during SHM or during the repair of oxidative damage that occurs during the proliferation of B cells in the GC may not be filled in efficiently by Y265C Pol β, leading to cell death. The presence of apoptotic or dying cells in the GCs could result in the release of antigen, resulting in positive selection of GC B cells that produce autoantibodies. This suggestion is supported by studies showing that mice with defective clearance of apoptotic cells develop lupus-like disease (Bickerstaff et al., 1999; Hanayama et al., 2004; Napirei et al., 2000). We suggest that in *POLB*$^{Y265C/C}$ mice, the large amount of apoptotic cells in GCs could overwhelm the apoptotic clearance machinery, thereby escaping clearance and being used for positive selection of autoreactive B cells. It is also possible that the increased SHM generates autoreactivity by targeting IgG-expressing memory B cells reentering the GC as a result of chronic exposure to self-antigen (Köhler et al., 2008; Meffre and Wardemann, 2008). Finally, it is possible that extrafollicular B cells could play a role in the generation of autoantibodies, as described for the MRL/lpr mouse model of SLE (Teichmann et al., 2010).

Aberrant DNA Repair and Autoimmunity

Previous work has shown that mutations of the *TREX1* DNA repair gene in humans are also associated with SLE (Stetson et al., 2008), but there is no evidence that these proteins act during the immunological processes of V(D)J, CSR, and SHM. Our findings demonstrate that a balance of hypermutation and

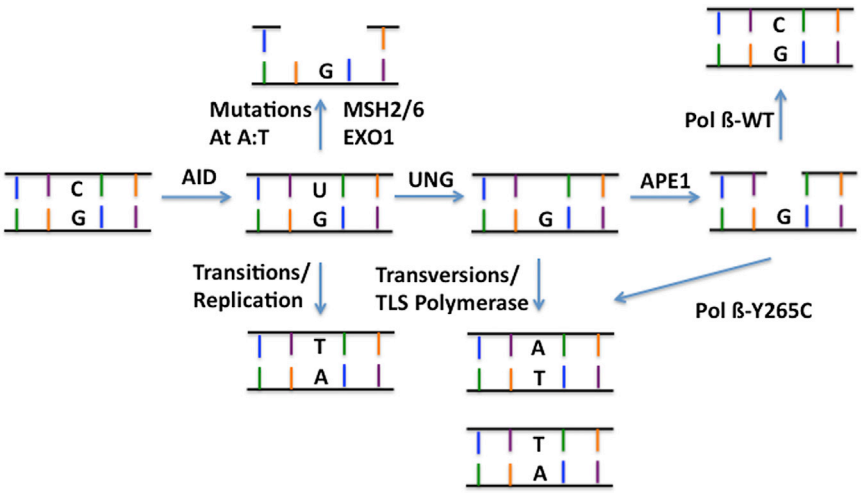

Figure 7. Y265C Permits Highly Error-Prone SHM, Resulting in Autoimmunity

After deamination of cytosine by AID, replication can occur, resulting in transitions. Alternatively, the mismatch repair pathway can bind to the U:G mismatch and recruit Exo 1, resulting in mutations at A:T base pairs. A third possibility is that APE1 incises the DNA at the AP site, resulting in a single nucleotide gap that is normally filled in by Pol β. However, in the presence of Y265C Pol β, the gap is filled inefficiently or not at all, leading to translesion synthesis and increased mutagenesis.

error-free BER during SHM is critical for the prevention of autoimmune disease. Our results do not rule out the possibility of other mechanisms that are not B cell intrinsic. For example, many cell types utilize Pol β Y265C during BER, and the accumulation of BER intermediates in these cells could lead to alterations in a variety of tissues, such as the gut epithelial barrier (including stem cells). Any resulting mucosal alterations could drive expansion of autoreactive clones. The results of our study suggest that mutations in DNA repair genes associated with immunological processes could lead to the development of autoimmune disease, including SLE.

EXPERIMENTAL PROCEDURES

Strain and Genotyping of Mice

Hybrid (129/Sv and C57BL/6) mice of both sexes were used for this study. All work with mice was carried out with oversight by the Yale University Institutional Animal Care and Use Committee.

Skin Histology

Skin tissues were fixed in histological 10% formalin solution fixative (Sigma-Aldrich) and embedded in paraffin. Skin sections were analyzed by a dermatopathologist.

Detection and Scoring of ANAs

ANAs were tested by immunofluorescence using human epithelial (Hep-2) cells on 12-well slides (Diasorin).

Histology and Scoring of Kidney Lesions

Tissues from mice were isolated and fixed in histological 10% formalin solution fixative (Sigma-Aldrich), and embedded in paraffin. Hematoxylin and eosin-stained tissues were evaluated as described in the Supplemental Experimental Procedures.

Immunohistochemistry

Details regarding immunohistochemistry are described in Supplemental Experimental Procedures.

Analysis of SHM

Genomic DNA was extracted from B220^{+}PNA^{high} cells obtained from Peyer's patches of two nonimmunized mice that were 3.5–5 months of age, and analyzed as described previously (Jolly et al., 1997; McDonald et al., 2003; Maccarthy et al., 2009).

Preparation of Genomic DNA, PCR Amplification, and Analysis of VDJ Recombination Sequences

Genomic DNA was prepared from B220^{+} IgM^{-} cells from spleen and bone marrow of three to five 3-week-old mice and analyzed as described in Supplemental Experimental Procedures (Gilfillan et al., 1993; Komori et al., 1993).

ELISA

ELISA 96-well plates were coated overnight at 4°C with the appropriate antisera and analyzed as described in Supplemental Experimental Procedures.

SUPPLEMENTAL INFORMATION

Supplemental Information includes Supplemental Experimental Procedures and four figures and can be found with this article online at http://dx.doi.org/10.1016/j.celrep.2013.12.017.

ACKNOWLEDGMENTS

This research was supported by grant ES019179 from the National Institute of Environmental Health Sciences.

Received: July 22, 2013
Revised: October 16, 2013
Accepted: December 11, 2013
Published: January 2, 2014

REFERENCES

Alt, F.W., Zhang, Y., Meng, F.L., Guo, C., and Schwer, B. (2013). Mechanisms of programmed DNA lesions and genomic instability in the immune system. Cell *152*, 417–429.

Barnes, D.E., and Lindahl, T. (2004). Repair and genetic consequences of endogenous DNA base damage in mammalian cells. Annu. Rev. Genet. *38*, 445–476.

Bertocci, B., De Smet, A., Weill, J.-C., and Reynaud, C.-A. (2006). Nonoverlapping functions of DNA polymerases mu, lambda, and terminal deoxynucleotidyltransferase during immunoglobulin V(D)J recombination in vivo. Immunity *25*, 31–41.

Bickerstaff, M.C., Botto, M., Hutchinson, W.L., Herbert, J., Tennent, G.A., Bybee, A., Mitchell, D.A., Cook, H.T., Butler, P.J., Walport, M.J., and Pepys, M.B. (1999). Serum amyloid P component controls chromatin degradation and prevents antinuclear autoimmunity. Nat. Med. *5*, 694–697.

Chagovetz, A.M., Sweasy, J.B., and Preston, B.D. (1997). Increased activity and fidelity of DNA polymerase beta on single-nucleotide gapped DNA. J. Biol. Chem. *272*, 27501–27504.

Clairmont, C.A., Narayanan, L., Sun, K.W., Glazer, P.M., and Sweasy, J.B. (1999). The Tyr-265-to-Cys mutator mutant of DNA polymerase beta induces a mutator phenotype in mouse LN12 cells. Proc. Natl. Acad. Sci. USA *96*, 9580–9585.

Di Noia, J.M., and Neuberger, M.S. (2007). Molecular mechanisms of antibody somatic hypermutation. Annu. Rev. Biochem. *76*, 1–22.

Furukawa, F., Tanaka, H., Sekita, K., Nakamura, T., Horiguchi, Y., and Hamashima, Y. (1984). Dermatopathological studies on skin lesions of MRL mice. Arch. Dermatol. Res. *276*, 186–194.

Gilfillan, S., Dierich, A., Lemeur, M., Benoist, C., and Mathis, D. (1993). Mice lacking TdT: mature animals with an immature lymphocyte repertoire. Science *261*, 1175–1178.

Gu, H., Marth, J.D., Orban, P.C., Mossmann, H., and Rajewsky, K. (1994). Deletion of a DNA polymerase beta gene segment in T cells using cell type-specific gene targeting. Science *265*, 103–106.

Guo, W., Smith, D., Aviszus, K., Detanico, T., Heiser, R.A., and Wysocki, L.J. (2010). Somatic hypermutation as a generator of antinuclear antibodies in a murine model of systemic autoimmunity. J. Exp. Med. *207*, 2225–2237.

Hanayama, R., Tanaka, M., Miyasaka, K., Aozasa, K., Koike, M., Uchiyama, Y., and Nagata, S. (2004). Autoimmune disease and impaired uptake of apoptotic cells in MFG-E8-deficient mice. Science *304*, 1147–1150.

Jolly, C.J., Klix, N., and Neuberger, M.S. (1997). Rapid methods for the analysis of immunoglobulin gene hypermutation: application to transgenic and gene targeted mice. Nucleic Acids Res. *25*, 1913–1919.

Jonsson, R., Tarkowski, A., Bäckman, K., Holmdahl, R., and Klareskog, L. (1987). Sialadenitis in the MRL-l mouse: morphological and immunohistochemical characterization of resident and infiltrating cells. Immunology *60*, 611–616.

Köhler, F., Hug, E., Eschbach, C., Meixlsperger, S., Hobeika, E., Kofer, J., Wardemann, H., and Jumaa, H. (2008). Autoreactive B cell receptors mimic autonomous pre-B cell receptor signaling and induce proliferation of early B cells. Immunity *29*, 912–921.

Komori, T., Okada, A., Stewart, V., and Alt, F.W. (1993). Lack of N regions in antigen receptor variable region genes of TdT-deficient lymphocytes. Science *261*, 1171–1175.

Lavoie, T.N., Lee, B.H., and Nguyen, C.Q. (2011). Current concepts: mouse models of Sjögren's syndrome. J. Biomed. Biotechnol. *2011*, 549107.

Liu, M., and Schatz, D.G. (2009). Balancing AID and DNA repair during somatic hypermutation. Trends Immunol. *30*, 173–181.

Ma, Y., Lu, H., Tippin, B., Goodman, M.F., Shimazaki, N., Koiwai, O., Hsieh, C.L., Schwarz, K., and Lieber, M.R. (2004). A biochemically defined system for mammalian nonhomologous DNA end joining. Mol. Cell *16*, 701–713.

Maccarthy, T., Roa, S., Scharff, M.D., and Bergman, A. (2009). SHMTool: a webserver for comparative analysis of somatic hypermutation datasets. DNA Repair (Amst.) *8*, 137–141.

Maul, R.W., and Gearhart, P.J. (2010). AID and somatic hypermutation. Adv. Immunol. *105*, 159–191.

McDonald, J.P., Frank, E.G., Plosky, B.S., Rogozin, I.B., Masutani, C., Hanaoka, F., Woodgate, R., and Gearhart, P.J. (2003). 129-derived strains of mice are deficient in DNA polymerase iota and have normal immunoglobulin hypermutation. J. Exp. Med. *198*, 635–643.

Meffre, E., and Wardemann, H. (2008). B-cell tolerance checkpoints in health and autoimmunity. Curr. Opin. Immunol. *20*, 632–638.

Napirei, M., Karsunky, H., Zevnik, B., Stephan, H., Mannherz, H.G., and Möröy, T. (2000). Features of systemic lupus erythematosus in Dnase1-deficient mice. Nat. Genet. *25*, 177–181.

Norris, D.A., and Lee, L.A. (1985). Pathogenesis of cutaneous lupus erythematosus. Clin. Dermatol. *3*, 20–35.

Opresko, P.L., Sweasy, J.B., and Eckert, K.A. (1998). The mutator form of polymerase beta with amino acid substitution at tyrosine 265 in the hinge region displays an increase in both base substitution and frame shift errors. Biochemistry *37*, 2111–2119.

Radic, M., Herrmann, M., van der Vlag, J., and Rekvig, O.P. (2011). Regulatory and pathogenetic mechanisms of autoantibodies in SLE. Autoimmunity *44*, 349–356.

Rajewsky, K., Förster, I., and Cumano, A. (1987). Evolutionary and somatic selection of the antibody repertoire in the mouse. Science *238*, 1088–1094.

Senejani, A.G., Dalal, S., Liu, Y., Nottoli, T.P., McGrath, J.M., Clairmont, C.S., and Sweasy, J.B. (2012). Y265C DNA polymerase beta knockin mice survive past birth and accumulate base excision repair intermediate substrates. Proc. Natl. Acad. Sci. USA *109*, 6632–6637.

Sheng, Y.J., Gao, J.P., Li, J., Han, J.W., Xu, Q., Hu, W.L., Pan, T.M., Cheng, Y.L., Yu, Z.Y., Ni, C., et al. (2011). Follow-up study identifies two novel susceptibility loci PRKCB and 8p11.21 for systemic lupus erythematosus. Rheumatology (Oxford) *50*, 682–688.

Stavnezer, J., Guikema, J.E., and Schrader, C.E. (2008). Mechanism and regulation of class switch recombination. Annu. Rev. Immunol. *26*, 261–292.

Stetson, D.B., Ko, J.S., Heidmann, T., and Medzhitov, R. (2008). Trex1 prevents cell-intrinsic initiation of autoimmunity. Cell *134*, 587–598.

Teichmann, L.L., Ols, M.L., Kashgarian, M., Reizis, B., Kaplan, D.H., and Shlomchik, M.J. (2010). Dendritic cells in lupus are not required for activation of T and B cells but promote their expansion, resulting in tissue damage. Immunity *33*, 967–978.

Victora, G.D., and Nussenzweig, M.C. (2012). Germinal centers. Annu. Rev. Immunol. *30*, 429–457.

Washington, S.L., Yoon, M.S., Chagovetz, A.M., Li, S.X., Clairmont, C.A., Preston, B.D., Eckert, K.A., and Sweasy, J.B. (1997). A genetic system to identify DNA polymerase beta mutator mutants. Proc. Natl. Acad. Sci. USA *94*, 1321–1326.

Weigert, M.G., Cesari, I.M., Yonkovich, S.J., and Cohn, M. (1970). Variability in the lambda light chain sequences of mouse antibody. Nature *228*, 1045–1047.

Wellmann, U., Letz, M., Herrmann, M., Angermüller, S., Kalden, J.R., and Winkler, T.H. (2005). The evolution of human anti-double-stranded DNA autoantibodies. Proc. Natl. Acad. Sci. USA *102*, 9258–9263.

Wu, X., and Stavnezer, J. (2007). DNA polymerase beta is able to repair breaks in switch regions and plays an inhibitory role during immunoglobulin class switch recombination. J. Exp. Med. *204*, 1677–1689.

Zeller, T., Wild, P., Szymczak, S., Rotival, M., Schillert, A., Castagne, R., Maouche, S., Germain, M., Lackner, K., Rossmann, H., et al. (2010). Genetics and beyond—the transcriptome of human monocytes and disease susceptibility. PLoS ONE *5*, e10693.